



# University of HUDDERSFIELD

## University of Huddersfield Repository

Bray, Andrew W., Stewart, Douglas I., Courtney, Ronan, Rout, Simon P., Humphreys, Paul, Mayes, William M. and Burke, Ian T.

Sustained Bauxite Residue Rehabilitation with Gypsum and Organic Matter 16 years after Initial Treatment

### Original Citation

Bray, Andrew W., Stewart, Douglas I., Courtney, Ronan, Rout, Simon P., Humphreys, Paul, Mayes, William M. and Burke, Ian T. (2018) Sustained Bauxite Residue Rehabilitation with Gypsum and Organic Matter 16 years after Initial Treatment. *Environmental Science and Technology*, 52 (1). pp. 152-161. ISSN 0013-936X

This version is available at <http://eprints.hud.ac.uk/id/eprint/34178/>

The University Repository is a digital collection of the research output of the University, available on Open Access. Copyright and Moral Rights for the items on this site are retained by the individual author and/or other copyright owners. Users may access full items free of charge; copies of full text items generally can be reproduced, displayed or performed and given to third parties in any format or medium for personal research or study, educational or not-for-profit purposes without prior permission or charge, provided:

- The authors, title and full bibliographic details is credited in any copy;
- A hyperlink and/or URL is included for the original metadata page; and
- The content is not changed in any way.

For more information, including our policy and submission procedure, please contact the Repository Team at: [E.mailbox@hud.ac.uk](mailto:E.mailbox@hud.ac.uk).

<http://eprints.hud.ac.uk/>

1 **Sustained Bauxite Residue Rehabilitation with Gypsum and Organic**  
2 **Matter 16 years after Initial Treatment**

3 Andrew W. Bray <sup>a\*</sup>, Douglas I. Stewart <sup>b</sup>, Ronan Courtney <sup>c</sup>, Simon P. Rout <sup>d</sup>,  
4 Paul N. Humphreys <sup>d</sup>, William M. Mayes <sup>e</sup>, Ian T. Burke <sup>a</sup>

5 <sup>a</sup> School of Earth and Environment, University of Leeds, Leeds LS2 9JT, UK

6 <sup>b</sup> School of Civil Engineering, University of Leeds, Leeds LS2 9JT, UK

7 <sup>c</sup> Department of Biological Sciences & The Bernal Institute, University of Limerick, Limerick,  
8 Ireland

9 <sup>d</sup> Department of Chemical and Biological Sciences, University of Huddersfield, Huddersfield HD1  
10 3DH, UK

11 <sup>e</sup> School of Environmental Sciences, University of Hull, Hull HU6 7RX, UK

12 \* Email for correspondence: a.w.bray@leeds.ac.uk

13

14

15

16

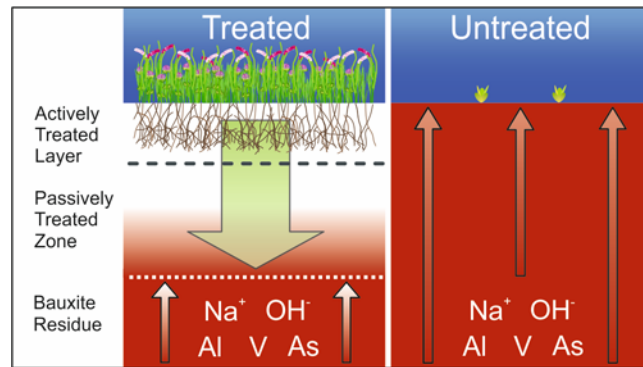
17

18 Prepared for *Environmental Science and Technology*

19 Word Count: 5796 (+ 1200 in tables and figures)

20

21 **Graphical Abstract**



22

23

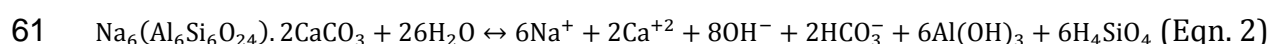
## 24 **Abstract**

25           Bauxite residue is a high volume by-product of alumina manufacture which is  
26 commonly disposed of in purpose-built bauxite residue disposal areas (BRDAs). Natural  
27 waters interacting with bauxite residue are characteristically highly alkaline, and have  
28 elevated concentrations of Na, Al, and other trace metals. Rehabilitation of BRDAs is  
29 therefore often costly and resource/infrastructure intensive. Data is presented from  
30 three neighbouring plots of bauxite residue that was deposited twenty years ago. One  
31 plot was amended 16 years ago with process sand, organic matter, gypsum, and seeded  
32 (fully treated), another plot was amended 16 years ago with process sand, organic matter,  
33 and seeded (partially treated), and a third plot was left untreated. These surface  
34 treatments lower alkalinity and salinity, and thus produce a substrate more suitable for  
35 biological colonisation from seeding. The reduction of pH leads to much lower Al, V and  
36 As mobility in the actively treated residue and the beneficial effects of treatment extend  
37 passively 20-30 cm below the depth of the original amendment. These positive  
38 rehabilitation effects are maintained after 2 decades due to the presence of an active and  
39 resilient biological community. This treatment may provide a lower cost solution to BRDA  
40 end of use closure plans and orphaned BRDA rehabilitation.

## 41 Introduction

42 Globally, >100 million tonnes of alumina is produced annually.<sup>1</sup> Producing 1 tonne  
43 of alumina generates 1-2 tonnes of bauxite residue (known as “red mud”). The residue  
44 varies with ore type, but all are alkaline, sodic, and contain similar minerals. In the Bayer  
45 process bauxite ore is digested with NaOH at high temperature and pressure which  
46 results in recrystallization of iron oxides present. Silica is a common impurity, which is  
47 removed from solution by precipitation of a range of characteristic Na- and Ca-  
48 aluminosilicate phases (e.g. sodalite and cancrinite).<sup>2,3</sup> These “desilication products”  
49 reside predominantly in the fine fraction. Residual aluminium (oxy)hydroxide phases,  
50 quartz, zircon and titanium oxides (e.g. rutile and perovskite) also occur in the residues.<sup>2,3</sup>

51 Bauxite residue has few uses (cement, iron and steel production, construction  
52 materials) and most is sent to bauxite residue disposal areas (BDRAs).<sup>4</sup> The liquid from  
53 bauxite residue is very alkaline (pH 11-13) and contains abundant sodium.<sup>5-7</sup> Subsequent  
54 dissolution of desilication products such as sodalite (Eqn 1.) and cancrinite (Eqn 2), along  
55 with associated amorphous secondary phases, generates further alkalinity and releases  
56 sodium in the long term.<sup>8-10</sup> Trace elements in bauxite, such as V and As, become  
57 concentrated in the residue, and are often hosted in surface complexes and secondary  
58 phases.<sup>10-14</sup> This can be environmentally problematic as Al, V, and As form aqueous  
59 oxyanions in alkaline conditions which sorb poorly to sediments<sup>15,16</sup>.



62 When left untreated, bauxite residue is infiltrated by CO<sub>2</sub> and the formation of  
63 aqueous and solid carbonate consumes OH<sup>-</sup>, lowering pH.<sup>17-19</sup> The depth to which this

64 process can act within bauxite residue is controlled by the rate of in-gassing and diffusion  
65 of CO<sub>2</sub>. These process can be enhanced by gypsum addition, providing excess Ca<sup>2+</sup> for  
66 precipitation of carbonate.<sup>20</sup> These reactions occur rapidly at high pH and can eventually  
67 buffer the pH to 7.5-8.5.<sup>17,21</sup> Previous work has shown that gypsum addition can also  
68 decrease the mobility of trace metals and Al in bauxite residue effected soils.<sup>17,21</sup> Other  
69 approaches to decrease bauxite residue salinity and alkalinity, such as treatment with  
70 acid<sup>22</sup> and seawater,<sup>23</sup> tend to only neutralise the aqueous, not the solid alkalinity  
71 generating phases. Ion exchange resins,<sup>24</sup> and bipolar-membranes electrodialysis<sup>25</sup> have  
72 been used to increase the longevity of treatment, yet these approaches rely on continued  
73 management and the utilisation of products by an active refinery. As such, common end-  
74 of-use practice is to cap BRDAs with an impermeable layer, cover with topsoil, and  
75 revegetate. The costs “cap and cover” approaches are high (e.g. 100k €/ha has been  
76 estimated for the BRDA in this study). However abandoning BRDAs without surface cover  
77 may lead to problems with long term water infiltration and dust formation.

78 Over the last 15 years Courtney and others have examined the effect of coarse  
79 fraction bauxite residue (process sand), gypsum, and organic matter on the revegetation  
80 of bauxite residue at Aughinish Alumina Refinery BRDA, Ireland.<sup>26-36</sup> These studies have  
81 assessed site rehabilitation by investigating macro- and microbiology, nutrient  
82 availability, and the chemical nature of the substrate. Beneficial effects from bio-  
83 rehabilitation have also been reported elsewhere.<sup>37,38</sup> Yet, little is known of the longevity  
84 and reliability of such surface treatments. Lack of long term data, and poorly constrained  
85 audit trails regarding treatment and planting histories, can limit their viability in BRDA  
86 closure plans. The objective of this study was to assess the long term effects of a surface  
87 treatment to bauxite residue. Here we report the chemical and mineralogical data

88 sampled from depth profiles of bauxite residue nearly two decades after initial treatment,  
89 and evaluate the ability of these treatments to provide sustained rehabilitation of the  
90 substrate and associated fluid.

## 91 **Methods**

92           In September 2015 trial pits were dug to ~60 cm in a BRDA located in a European  
93 Union member state with a temperate oceanic climate (average annual rainfall ~1m). At  
94 this site bauxite residue was deposited into a 3m deep disposal cell in 1995, and  
95 subsequently treated to encourage revegetation in 1999. Therefore, sampling was  
96 undertaken 20 years after deposition and 16 years after treatment.<sup>31</sup> Three plots within  
97 the BRDA were investigated. The fully treated plot was amended with gypsum (3% w/w  
98 rotavated-in to a depth 30 cm), process sand (10% w/w rotavated-in to a depth of 30cm),  
99 spent mushroom compost (80t Ha<sup>-1</sup> rotavated-in to a depth of 20cm), and seeded with a  
100 grassland mix (*Agrostis stolonifera*, *Holcus lanatus*, *Lolium perenne*, *Trifolium repens*, and  
101 *Trifolium pratense*; 100 kg/ha).<sup>31</sup> The partially treated plot was amended only with  
102 process sand, spent mushroom compost, and then seeded. The third plot was left  
103 untreated. Samples of bauxite residue were collected to a depth of 50 cm from the trial  
104 pits in each of three different treatment zones. Duplicate sample profiles in each plot were  
105 taken from two separate clean vertical surfaces of trial pits and stored in polypropylene  
106 tubes. The dual depth profiles were sampled to observe and account for heterogeneity in  
107 the residue.

108           Field moist samples were stored at 5 °C before aqueous extraction for major and  
109 trace metals. 10 gram subsamples were mixed with 10 mL of ultrapure water (18.5 MΩ)  
110 and shaken at room temperature for seven days. The solution pH was measured using a  
111 Thermo Scientific Orion ROSS Ultra electrode calibrated with 4.00, 7.00, and 10.00  
112 buffers (Fisher Scientific). 1 gram field moist subsamples were mixed with 10 mL of a 0.1  
113 M Na<sub>2</sub>HPO<sub>4</sub> in 0.01 M NaOH and shaken at room temperature for 7 days for phosphate  
114 extraction of metal oxyanions. Supernatant solutions from both the water and phosphate



115 extractions were filtered through 0.2  $\mu\text{m}$  disposable polyethersulfone filters (Sartorius)  
116 and acidified in 5%  $\text{HNO}_3$  for subsequent aqueous analysis by ICP-OES (Thermo Fisher  
117 iCAP 7400 Radial ICP-OES) (see SI section S1 for further details).

118 Further 10 g field moist subsamples were also dried at 105  $^\circ\text{C}$  for 24 hours to  
119 determine residue water content and for subsequent analysis by X-ray diffraction  
120 (XRD; Bruker D8 Advance diffractometer, 12 min. scans, 2 to 70 $^\circ$   $2\theta$ ), X-ray fluorescence  
121 (XRF, Olympus Innovex X-5000 XRF analyser) and total carbon analysis (TC; LECO SC-  
122 144DR carbon analyser). The crystalline phases present were determined from XRD  
123 patterns by peak fitting using EVA (version 3.0, Bruker), and semi-quantitative relative  
124 proportions were calculated by Rietveld refinement using Topas (version 4.2, Bruker).  
125 Total organic carbon (TOC) were measured after a 24 hour digestion in 10% HCl at room  
126 temperature. Total inorganic carbon (TIC) was calculated from TC and TOC  
127 measurements.

128 Acid soluble inorganic and organic substances (AIC and AOC) were determined in  
129 12 samples after extraction with 2 M HCl (1 g soil in 5 mL of 2 M HCl for 3 days at 4  $^\circ\text{C}$ ).  
130 The extractant was then separated by centrifugation at 8000  $g$  for 10 min, pH neutralised  
131 by drop-wise addition of 2 M NaOH, evaporated to dryness; and finally the resulting solid  
132 dissolved in ultra-pure water at 1  $\text{g}\cdot\text{L}^{-1}$ .<sup>39</sup> Total carbon and total inorganic carbon in the  
133 extractant was determined using a Shimadzu total organic carbon analyser 5050A (LOD  
134 4  $\mu\text{g kg}^{-1}$ ).

135 Separate samples of bauxite residue were collected from beneath the exposed  
136 vertical surface of each trial pit using a clean spatula, and sealed in sterile polypropylene  
137 centrifuge tubes. These samples for DNA analysis were refrigerated within 4 hours and  
138 frozen within 48hrs. DNA was isolated from 0.5 g of each sample using the MPBio

139 FastDNA SPIN Kit for Soil. Isolated DNA mass from each sample was determined by Qubit  
140 dsDNA High Sensitivity assay on a Qubit Fluorometer (Life Technologies; further details  
141 of quantification are in SI Section S3). DNA samples were sent to the Centre for Genomic  
142 Research, University of Liverpool, where Illumina TruSeq adapters and indices were  
143 attached to DNA fragments in a two-step PCR amplification that targets the V4 hyper-  
144 variable region of the 16s rRNA gene,<sup>40</sup> and the result was sequenced on the MiSeq  
145 platform. Reads were processed using the UPARSE pipeline<sup>41</sup> within the USEARCH  
146 software package (version 10, SI Section S3).<sup>42</sup> Sequence reads were allocated to  
147 operationally taxonomic units (OTUs) based on a minimum sequence identity of 97%  
148 between the putative OTU members, and then classified using the SILVA Living Tree  
149 Project 16s database, version 123.<sup>43</sup>

150           Difference in average element concentration between plot treatments (untreated,  
151 fully treated, and partially treated) was tested by ANCOVA (Analysis of Co-Variance)  
152 using a general linear model to assess difference in average concentrations across the  
153 treatments, with depth of sample as a co-variate. Pairwise comparisons were tested by  
154 post-hoc Tukey test using a significance level of  $p = 0.05$ . Statistical significance was  
155 expressed at  $p < 0.05$  and  $p < 0.001$  and the degrees of freedom for all tests varied  
156 between 19 and 64.

## 157 **Results**

### 158 *Sampling observations*

159 Both the fully treated and partially treated sites were vegetated with a variety of  
160 perennial grasses (*Holcus lanatus*), trifoliolate clovers (*Trifolium pratense*), and occasional  
161 small shrubs (*Salix* spp.; Fig. S1), as has been described previously.<sup>31</sup> The untreated plot  
162 was largely unvegetated with one or two areas of stunted grasses (Fig. S1). The root zone  
163 of the fully treated and partially treated sites extended approximately 15 cm beneath the  
164 surface, and below 20cm the substrate had the appearance of dewatered bauxite residue  
165 with little change in appearance to 50 cm depth. The untreated profile had no root zone  
166 and at all depths had a very similar appearance to the residue in the other profiles at  
167 depths below 20 cm. The bottom of the untreated pit filled with leachate to a depth of  
168 about 10 cm after 2 hours.

### 169 *Substrate characteristics*

170 The pH of the untreated residue was 10.2 at the surface and steadily increased to  
171 12.0 at a depth of 50 cm (Fig. 1; SI Table S2). The pH of the treated plots were notably and  
172 significantly lower ( $p < 0.001$ ; Table S3). The fully treated residue was pH 7.6 at the  
173 surface, and increased steadily to a value of 9.6 at a depth of 50 cm. The pH value of the  
174 partially treated residue was 7.6 at the surface, increased steadily to a value of 10.8 at a  
175 depth of 50 cm, and was not significantly different from the fully treated residue ( $p > 0.05$ ;  
176 Fig 2; Table S2-3).

177 The amount of sodium available to aqueous extraction of the untreated bauxite  
178 residue was  $\sim 900 \text{ mg kg}^{-1}$  of bauxite residue, and with exception of concentrations at the  
179 surface and at 50 cm there was little variation with depth (Fig. 1, Table S2). The amount

180 of Na that could be extracted from the fully treated and partially treated samples  
181 demonstrated no trend with depth and were not significantly different from each other  
182 ( $p > 0.05$ ; Table S3). Fully and partially treated residue contained concentrations  
183 approximately 10-15 % of those extracted from the untreated residue at the same depth  
184 ( $p < 0.001$ ; Fig. 1; Table S2-3). The concentration of silicon available to aqueous extraction  
185 in the untreated bauxite residue was  $5 \text{ mg kg}^{-1}$ , and apart from the measured  
186 concentration from 50 cm there was minimal variation with depth (Fig. 1, Table S2). Si  
187 concentrations extracted from fully treated and partially treated bauxite residue were  $\sim 4$   
188  $\text{mg kg}^{-1}$  below 5 cm, and  $\sim 13 \text{ mg kg}^{-1}$  above 5cm, there was no significant difference  
189 between fully, partially, or untreated residue ( $p > 0.05$ ; Fig. 1; Table S2-3). Calcium  
190 concentrations from the aqueous extraction of untreated bauxite residue ranged from 3  
191  $\text{mg kg}^{-1}$  at the surface to below the limit of detection at 50 cm ( $0.11 \text{ mg kg}^{-1}$ ) (Fig. 1, Table  
192 S2). In contrast Ca concentrations from fully treated and partially treated samples were  
193 significantly different to the untreated residue ( $p < 0.001$ ; Table S3),  $143 \text{ mg kg}^{-1}$  at the  
194 surface decreasing to  $\sim 10 \text{ mg kg}^{-1}$  at 20 cm, with further slight concentration decrease to  
195  $\sim 2 \text{ mg kg}^{-1}$  at 50 cm with no significant difference between treatments ( $p > 0.005$ ; Fig. 1;  
196 Table S2-3).

197         The aluminium concentration available to aqueous extraction in untreated bauxite  
198 residue was  $\sim 10 \text{ mg kg}^{-1}$  at the surface which increases steadily with depth to  $\sim 65 \text{ mg}$   
199  $\text{kg}^{-1}$  at 50 cm (Fig 2. Table S2). Conversely, Al concentrations available in fully and  
200 partially treated samples were significantly different ( $p < 0.001$ , Table S3) and near the  
201 detection limit ( $0.09 \text{ mg kg}^{-1}$ ) at all depths, apart from at 30-50 cm where Al  
202 concentrations were  $1\text{-}10 \text{ mg kg}^{-1}$  (Fig 2. Table S2). There was no significant difference  
203 between treatments ( $p > 0.05$ , Table S3). The amount of vanadium available to aqueous

204 extraction from untreated bauxite residue was  $\sim 5 \text{ mg kg}^{-1}$  and did not vary greatly with  
205 depth (Fig 2. Table S2). Aqueous extractable V in fully treated and partially treated  
206 samples were near detection limit at the surface ( $0.03 \text{ mg kg}^{-1}$ ) and increased gradually  
207 with depth to maximum concentrations of  $3.9 \text{ mg kg}^{-1}$  at 50 cm, significantly different  
208 from untreated residue ( $p < 0.001$ , Table S3) but not significantly different between fully  
209 and partially treated residue ( $p > 0.05$ ; Fig 2; Table S2-3). Aqueous available arsenic  
210 concentrations from untreated bauxite residue were highest at the surface ( $0.3 \text{ mg kg}^{-1}$ )  
211 and decrease with depth to  $0.9 \text{ mg kg}^{-1}$  at 50 cm depth (Fig 2. Table S2). With the  
212 exception of one sample, all measurements of aqueous extractable As from fully treated  
213 and partially treated bauxite residue were below detection limit ( $0.045 \text{ mg kg}^{-1}$ ) and  
214 significantly different from the untreated residue ( $p < 0.001$ ; Fig 2; Table S2-3).  
215 Extraction at high pH using disodium phosphate demonstrated substantial  
216 concentrations of Al, V, and As were available in all bauxite residue treatments. Phosphate  
217 extractable Al concentrations from all treatments are generally all  $25\text{-}50 \text{ mg kg}^{-1}$  at all  
218 depths (no significant differences between treatments;  $p > 0.05$ ; Table S2-3). V  
219 concentrations from the phosphate extraction of untreated bauxite residue range from  
220  $30\text{-}75 \text{ mg kg}^{-1}$  at the surface to  $30 \text{ mg kg}^{-1}$  at 50 cm depth (Fig 2. Table S2). Phosphate  
221 available V from fully treated and partially treated samples was lowest at the surface  
222 ( $\sim 15 \text{ mg kg}^{-1}$ ) and increases with depth to  $\sim 75 \text{ mg kg}^{-1}$  at 50 cm, but with no significant  
223 differences between untreated, fully treated, or partially treated residue ( $p > 0.05$ ; Fig 2.  
224 Table S2-3). Arsenic concentrations extracted from untreated bauxite residue at high pH  
225 with phosphate are  $\sim 2.5 \text{ mg kg}^{-1}$  at the surface and decrease to  $< 1 \text{ mg kg}^{-1}$  at 50 cm (Fig  
226 2. Table S2). Phosphate extractable As from fully treated and partially treated samples  
227 increase with depth from  $\sim 1 \text{ mg kg}^{-1}$  at the surface to  $\sim 2.5 \text{ mg kg}^{-1}$  at 50 cm (Fig 2. Table  
228 S2). Phosphate extractable As from fully treated and partially treated residue were

229 significantly different ( $p < 0.05$ ), though neither were significantly different from the  
230 untreated residue ( $p > 0.05$ ; Table S3).

231         The water content of the residue (weight of water as % of dry weight) at both the  
232 fully and partially treated sites was over 50% near the surface, exhibited a minimum of  
233 ~30 % at approximately 10 cm, and then increased to between 35 and 45 % at depths  
234 below 20 cm (Table S2). In contrast the water content in the untreated profile was 35%  
235 near to the surface, exhibited a maximum value of ~50 % at 10cm, and then decreased  
236 slightly to 40 % at depths below 30 cm. Water in the untreated residue was significantly  
237 different to fully treated residue ( $p < 0.001$ ), but not significantly different from partially  
238 treated residue ( $p > 0.05$ ; Table S3)

239         The bulk mineralogy of bauxite residue from all plots were largely similar and  
240 consist of 40-45% iron oxy-hydroxides, 20-30% aluminium oxy-hydroxides, 20-30%  
241 titanium oxides, and 10-15% feldspathoids (Table 1, Table S4). At the untreated bauxite  
242 residue plot there were no differences in the relative proportions of each phase with  
243 depth. Variations in the relative proportions of phases within the residue as a function of  
244 depth and treatment were within the range of uncertainty of Rietveld refinement (5 %).  
245 The alkali generating feldspathoid and desilication product cancrinite was present at all  
246 depths in all treatment sites (Table 1, Table S4). There was little difference in the bulk  
247 elemental composition measured by XRF with either depth or treatment (Table S5). Fe,  
248 Al, Ca, Si and Ti were the most abundant oxides in present each site ( $36 \pm 3$ ,  $10 \pm 2$ ,  $15 \pm 2$ ,  
249  $5 \pm 1$  and  $4 \pm 1$  wt. % respectively). Carbon was most concentrated in the top 10 cm of the  
250 fully treated profile (Fig. 3), where TOC was approximately 2.5% and TIC was 1.5%.  
251 Below 10 cm there was no discernible difference in carbon content between the fully  
252 treated and untreated profiles. Samples of untreated bauxite had less than 0.5% TOC and

253 TIC at all depths. Acid extractable inorganic carbon (AIC) and organic carbon (AOC) was  
254 only detectable in the top 10 cm of the fully treated and untreated bauxite residue, and  
255 was below or at the limit of detection ( $<4 \mu\text{g kg}^{-1}$ ) in all other samples (Table S2).

256 DNA mass isolated per gram of sample demonstrated a strong vertical gradient  
257 and significant difference between the treated (fully treated and partially treated) and  
258 untreated sites (Fig. 3, Table S6). DNA was concentrated in the top 12 cm of the fully  
259 treated and partially treated sites where maximum concentrations were up to  $14.3 \mu\text{g g}^{-1}$   
260 <sup>1</sup>. The highest concentration of DNA in the untreated samples was  $2.3 \mu\text{g g}^{-1}$  in the near  
261 surface. Below 12 cm the DNA concentrations in the fully treated, partially treated and  
262 untreated residue were negligible.

263 Sufficient bacterial DNA was recovered from the fully treated substrate (2 cm),  
264 and partially treated substrate (2 and 5 cm) for Next Generation Sequencing (DNA  
265 recovery from the untreated substrate was insufficient). Nine phyla individually  
266 represented more the 1% of the population of each sample (Fig. S2, Table S7). At this  
267 taxonomic level, there was little difference between bacterial communities of the fully  
268 treated and partially treated substrate, with the most abundant phyla being  
269 Acidobacteria (37 % of reads), Actinobacteria (19 %), Proteobacteria (18 %), and  
270 Planctomycetes (14 %). The most abundant class within the Acidobacteria phylum was  
271 Acidobacteria Gp6 (48 % of Acidobacteria). Actinomycetales (74 %) was the most  
272 abundant order within the Actinobacteria phylum. Alphaproteobacteria (67 %) was the  
273 most abundant class within the Proteobacteria. 100 % of the Planctomycetes phylum  
274 mapped onto the Planctomycetaceae family.

275 The alpha diversity indices for each sample are shown in Table S8. Here we use  
276 Hill numbers<sup>44,45</sup> as robust bacterial diversity measures which account for the distortions

277 of rare taxa.<sup>44-47</sup>  $D_0^\alpha$ , the operational taxonomic unit (OTU) richness, ranges from ~1250  
278 to 3850, however this diversity index is very sensitive to rare taxa, and takes no account  
279 of OTU relative abundance. Indices that give a measure of the number of common ( $D_1^\alpha$ )  
280 and dominant OTUs ( $D_2^\alpha$ ; Table S8), converge across the samples, demonstrating similar  
281 diversity in the OTU populations. Common OTUs represent >79 % of total sequence reads  
282 in each sample, and dominant OTUs accounted for 51-62 % of total reads in each sample.

283



## 284 Discussion

### 285 *The geochemistry of 20 year old untreated bauxite residue*

286 Fresh bauxite residue is highly alkaline (pH 10–13), highly sodic (abundant mobile  
287 Na), contains abundant solid phase alkalinity (e.g. desalination products; 2-51%) and can  
288 also contain trace metals above threshold intervention levels.<sup>10,12,26,27,48-52</sup> The  
289 desilication products in fresh residue tend to have higher proportion of sodalite to  
290 cancrinite<sup>10</sup> however, with age sodalite can transform into cancrinite.<sup>53</sup> Initially the high  
291 pH and sodium contents are due to remnant NaOH from the Bayer Process. Previous work  
292 has shown that repeated replacement of pore water decreases the mass of fresh bauxite  
293 residue but does not alter final pH, Na<sup>+</sup>, Al(OH)<sub>4</sub><sup>-</sup>, CO<sub>3</sub><sup>2-</sup>, or OH<sup>-</sup> concentrations<sup>8</sup> due to the  
294 dissolution desilication products, and associated amorphous phases (Eqn 1, 2). When left  
295 untreated, the pH of bauxite residue is controlled by the balance between CO<sub>2</sub> infiltration  
296 from the atmosphere, and OH<sup>-</sup> production through desilication product dissolution.

297 20 years after deposition the measured pH of the untreated bauxite residue ranges  
298 from pH 10 at the surface to pH 12 at 50 cm. XRD analysis indicates that cancrinite was  
299 the primary desilication product present (Table S4). At the surface, CO<sub>2</sub> in-gassing, in  
300 combination with cancrinite dissolution, and associated amorphous Fe, Al, and Si phase  
301 solubility, buffers the pore fluids to approximately pH 10. Atmospheric CO<sub>2</sub> in-gassing  
302 appears to extend ~20 cm from the surface (Fig. 1). Below 20 cm the bauxite residue  
303 appears to be isolated from the atmosphere and dissolution of cancrinite results in higher  
304 pH ( $\geq 11.5$ ; Fig. 1). Cancrinite dissolution also controls long term Na availability (Eqn. 2),  
305 and results in aqueous available Na concentrations of ~900 mg kg<sup>-1</sup> in untreated bauxite  
306 residue after 20 years. However, dissolution of cancrinite appears to be incongruent at  
307 high pH. Cancrinite dissolution should produce equimolar concentrations of Na, Si, and

308 Al, (Eqn. 2) but the measured concentrations are far from stoichiometric (Fig. S3).  
309 Aqueous extractable Na concentrations from untreated samples are 100 to 400 times  
310 higher in concentration than extractable Si and 10 to 150 times the Al concentration,  
311 indicating a preferential retention of Si and Al in the solid phase.

312 This preferential retention of Al and Si in the solid phase is probably controlled by  
313 the precipitation of amorphous and crystalline secondary phases. At the highest pH  
314 measured, Al concentrations are close to equilibrium with gibbsite ( $\text{Al}(\text{OH})_3$ ) (Fig S2).  
315 The measured Al concentrations decrease as the pH decreases from 12 to 10, but exceeds  
316 concentrations in equilibrium with gibbsite. Over this pH range, Si concentrations are  
317 much lower than those expected for  $\text{SiO}_{2(\text{am})}$  equilibrium, suggesting an alternative  
318 solubility limiting phase. At high pH, with high Na concentrations, Al and Si can co-  
319 precipitate in amorphous cation-bridged alumino-silicate gels,<sup>54</sup> which may explain the  
320 low concentrations observed.

321 Sustained alkalinity generation throughout untreated bauxite residue is a concern  
322 because it may be associated with increased mobility of potentially toxic metal(oid)  
323 oxyanions such as Al, V, and As. Both V and As are reported to be present in bauxite  
324 residues primarily in the 5+ oxidation state as vanadate and arsenate species<sup>10,12</sup>, and  
325 are found as surface adsorbed species (V can also be associated with neoformed  
326 hydrogarnet phases such as Katoite).<sup>12</sup> Conversely, Al availability is usually controlled by  
327 the solubility of Al (oxy)hydroxide phases, which typically have much higher solubility at  
328 high pH (see discussion above).<sup>55</sup> In alkaline phosphate extractions both  $\text{OH}^-$  and  
329 phosphate ions compete strongly for available sorption sites and promote the mobility of  
330 metal oxyanions.<sup>14,20</sup> The results of these extractions, therefore, demonstrate that there  
331 is abundant V and As adsorbed to bauxite residue (Fig. 2). In the untreated samples,

332 where pH > 10, As and V sorb poorly to mineral surfaces,<sup>14-16,21,56-58</sup> which is why only 10  
333 and 15 % of the phosphate extractable As and V respectively were extractable water this  
334 fraction will be mobile in residue pore waters.

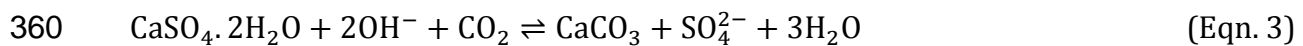
335 In summary, the bauxite residue from the untreated plot retains many of the  
336 characteristics of the fresh bauxite residue 20 years after deposition: high pH, a sizeable  
337 quantity of desilication products (particularly cancrinite), abundant available Na, high Al,  
338 V, and As concentrations, low organic carbon concentrations. Thus, untreated, it is an  
339 environment that is not conducive to spontaneous macro- or microorganism colonization  
340 through translocation.

341

#### 342 *Treated bauxite residue*

343 16 years after bauxite residue treatment with process sand, organic matter and  
344 gypsum significant pH reduction (2 units) was observed over a depth that extends at least  
345 30 cm below the actively treated surface layer (Fig. 1; Table S2). Aqueous sodium  
346 concentrations were an order of magnitude lower in the treated plots than untreated plot  
347 at all depths (Fig. 1; Table S2), and the availability of aluminium, vanadium, and arsenic  
348 were all lower in treated than untreated bauxite residue (Fig. 2; Table S2). These  
349 observations demonstrate that positive treatment effects observed in the short term are  
350 sustained, such as: improved permeability, particle aggregation, and drainage; pH  
351 neutralisation; decreased Na, Al, and Fe availability.<sup>28,29</sup> In natural soils, organic matter  
352 plays a key role in controlling particle aggregation,<sup>59-61</sup> and the application of spent  
353 mushroom compost may have improved residue structure. In highly alkaline conditions,  
354 organic matter dissolves and hydrolyses to form humic substances and lower molecular

355 weight organic anions.<sup>62-64</sup> This process lowers pH and releases organic bound nutrients  
356 to the local environment. Other studies have reported significant reduction in pH  
357 following organic matter application to bauxite residue.<sup>28,29,65,66</sup> Gypsum application  
358 enhances pH neutralisation by CO<sub>2</sub> in-gassing via the precipitation of CaCO<sub>3</sub>.<sup>20,21</sup> The net  
359 reaction for this mechanism is:



361 Increased CO<sub>2</sub> in-gassing and formation of dissolved carbonate species (supplementary  
362 information Eqns S2-7) can buffer the pH to 7.5-8, similar to natural alkaline soils, thus  
363 producing an environment less hostile to biological colonisation. At this site bauxite  
364 residue treatment with gypsum (in addition to process sand and organic matter) resulted  
365 in greater plant biomass in the first two years of growth,<sup>26-28</sup> and a more diverse and  
366 developed vegetation succession after 6 years (i.e. partial replacement of clover by more  
367 extensive grass cover and the establishment of small shrubs).<sup>31</sup> However, 16 years after  
368 treatment, there is no significant chemical or microbiological difference between the fully  
369 and partially treated substrate.

370 Long term alkalinity generation and sodium release in the 20 year old bauxite  
371 residue is controlled by cancrinite dissolution. Cancrinite dissolution kinetics as a  
372 function of pH is unreported in the literature, but the feldspathoids leucite and nepheline  
373 exhibit dissolution kinetics that decrease by an order of magnitude as pH decreases from  
374 12 to 7.<sup>67-70</sup> The dissolution kinetics of multioxide silicates, including aluminosilicates,  
375 are controlled by the solubilities of secondary phases,<sup>71</sup> thus it is inferred that these  
376 decreases in feldspathoid dissolution rate are linked to the solubilities of secondary  
377 aluminium and silicon phases. It is reasonable to expect cancrinite dissolution kinetics to  
378 vary with pH in a similar manner to other feldspathoids, decreasing by an order of

379 magnitude between pH 12 and 7. This suggests pH conditions established in treated  
380 bauxite residue from organic matter and gypsum addition decrease the rate of OH<sup>-</sup> and  
381 Na<sup>+</sup> production from the dissolution of cancrinite and associated secondary phases (Fig.  
382 1).

383 Aqueous extracted aluminium concentrations from partially and fully treated  
384 bauxite residue plotted as a function of pH (Fig. S3) fall on a line parallel to, but in  
385 between, the solubility lines of gibbsite and Al(OH)<sub>3</sub> (am). This is different to the trend  
386 observed for the untreated samples at higher pH, suggesting a different solubility  
387 controlling phase. Between pH 8 and 10 formation of dawsonite (NaAlCO<sub>3</sub>(OH)<sub>2</sub>) and an  
388 amorphous precursor to boehmite have been observed in bauxite residue treatment.<sup>12,72</sup>  
389 and may be the solubility controlling phases at this site. The phosphate extraction shows  
390 that there is abundant extractable Al, V, and As in both the partially and fully treated  
391 bauxite residue (Fig. 2; Table S2). However the aqueous extractions showed that nearer  
392 to neutral pH Al is secured in secondary phases, and the majority of V and As is sorbed to  
393 mineral surfaces<sup>14-16,21,56-58</sup> making Al, V, and As, much less available to aqueous solution  
394 (Fig. 2).

395

### 396 *Long term maintenance of beneficial conditions*

397 Rehabilitation of bauxite residue disposal areas by vegetation using the  
398 treatments described here is a pH dependant processes with benefits extending 20-30  
399 cm beyond the initial treatment depth. After 20 years of rainwater infiltration the  
400 alkalinity generating phases have not been exhausted, thus other processes must be  
401 controlling residue neutralisation. 16 years after treatment, the original additives are

402 largely unobservable, with little chemical difference remaining from the application of  
403 gypsum. This suggests that the development of resilient vegetation on bauxite residue,  
404 along with associated rhizosphere microorganisms, may drive long term stability and  
405 chemical safety of treated bauxite residue. The organic matter applied to the surface  
406 layers is only detected in small quantities (Fig. 3) and has likely been degraded and  
407 recycled into plants and microorganisms. The products of gypsum addition are minimal;  
408 calcite was undetectable by XRD, and there is only a slight accumulation of Ca and TIC  
409 towards the surface of both treated zones. Process sand was present in the surface layer  
410 when sampling but heterogeneously distributed and undetectable mineralogically by  
411 XRD and chemically by XRF.

412         The supply of H<sup>+</sup> ions to depth that is driving pH neutralisation in treated bauxite  
413 residue may be photosynthetic in origin. This can occur via a combination of three  
414 mechanisms: (a) enhanced CO<sub>2</sub> flux from plant roots and associated microorganism  
415 respiration; (b) organic matter degradation in the biologically active surface layer,  
416 producing low molecular weight organic acids; and (c) secretion of low molecular weight  
417 organic acids by plant roots and rhizospheric microorganisms. The carbon flux from  
418 atmosphere to rhizosphere is well documented in both the short (i.e. respiration), and  
419 medium terms (organic matter production).<sup>73</sup> Quantification of extracted DNA from both  
420 the treated plots suggests a zone of greater biological activity in the top 12 cm of treated  
421 bauxite residue (Fig. 3). DNA recovery is media dependent, with particle size and pH  
422 potentially affecting the efficiency of extraction. This uncertainty may over emphasise the  
423 gradient of biological activity with depth, and between treated and untreated samples.  
424 The extracted DNA concentrations from the top 12 cm of treated bauxite residue are  
425 within the range of extracted DNA concentrations from natural soils (very approximate

426 soil DNA concentrations range from 2.5 to 26.9  $\mu\text{g g}^{-1}$ ).<sup>74</sup> DNA recovery from this site's  
427 untreated bauxite residue was insufficient for Next-Generation Sequencing, however  
428 other workers have shown bauxite residue to contain alkali tolerant bacteria.<sup>75</sup>  
429 Sequenced DNA recovered from the root zone substrate of the fully and partially treated  
430 bauxite residue was dominated by the phyla Acidobacteria, Actinobacteria,  
431 Proteobacteria, and Planctomycetes. Natural soil root zone or rhizosphere bacterial  
432 communities frequently contain Actinobacteria, Bacteroidetes, Firmicutes, and  
433 Proteobacteria taxa,<sup>76-78</sup> which, with the exception of Firmicutes, are present in our  
434 treated bauxite residue (Figure S2, Table S7). Many taxa of Acidobacteria are known to  
435 be tolerant to high pH, and show increasing relative abundance with increasing pH from  
436 5.5 pH.<sup>79-82</sup> Many Planctomycetes taxa are halotolerant,<sup>83-87</sup> existing in freshwater,  
437 marine, and brackish environments. The presence of these phyla suggests the microbial  
438 communities in the fully and partially treated bauxite residue are in transition between a  
439 highly alkaline and saline residue microbiome, and a plant supported subsurface  
440 microbiome.

441 Surface treatment with process sand, gypsum, and organic matter is a stable,  
442 reliable, and safe solution to bauxite residue rehabilitation. Bauxite residue pH is  
443 neutralised,  $\text{Na}^+$  is less available, and metal oxyanions (Al, V, and As) are less mobile. The  
444 beneficial effects of treatment are long term and extend 20-30 cm beyond the depth of  
445 application. The formation a passively treated zone, which is  $\geq 20\%$  of the total disposal  
446 cell depth, is sufficient to separate the surface environments from the potentially highly  
447 alkaline, sodium rich, and trace metal containing residue at depth. The presence of  
448 alkalinity generating phases in both treated plots highlights the importance of  
449 maintaining a strong biologically active surface layer. Were this layer to be removed or

450 substantially disrupted, and its supply of acid neutralising molecules lost, the system  
451 would likely return to a high pH steady state, with high Na, Al, V, and As concentrations,  
452 similar to those observed in the untreated bauxite residue.

453           This is the first observation of a shallow surface layer of actively treated and  
454 vegetated residue producing passive positive rehabilitation effects into deeper layers.  
455 This rehabilitation is likely driven by biology activity at the surface and continues long  
456 after the original treatment constituents (gypsum, organic matter) have been depleted.  
457 Rehabilitation has resulted in a physical separation between deeper zones within the  
458 residue (potentially containing high alkalinity, sodium, and trace metals) and the bottom  
459 of the rooted zone at around 20 cm. Rehabilitation decreases the likelihood of plants  
460 being exposed to the negative characteristics of bauxite residue, and lowers the  
461 possibility of trace metal transfer into foliage and the wider ecosystem. The benefits of  
462 this surface treatment extend beyond the environmental; the cost of application is  
463 approximately 10k €/ha, whereas the cap and cover estimate for this BDRA is 100k €/ha.  
464 Gypsum application accounts for approximately 50-70 % of the total treatment cost, and  
465 assessment of its value for long term rehabilitation is important. Our results suggest the  
466 development of a healthy vegetation cover is key to long term stability of residue  
467 rehabilitation and previous work has demonstrated the role of gypsum in rapidly, and  
468 successfully establishing a resilient vegetation layer.<sup>26-28,31,32,35</sup> Gypsum application may,  
469 therefore, offer additional security in vegetation establishment, and the ultimate success  
470 and longevity of rehabilitation. However, 16 years after application there are no  
471 significant chemical benefits from gypsum addition. Our study demonstrates surface  
472 amendment of this nature is a viable closure option for active BRDAs and a particularly



473 good choice for rehabilitation of orphan sites where there is an acute need to protect the  
474 public and environment at the lowest possible costs.

#### 475 **Supporting Information**

476 Detailed aqueous analysis, DNA extraction, quantification, and post sequence processing  
477 methods. Stepwise reactions of gypsum promoted CaCO<sub>3</sub> precipitation and pH  
478 neutralisation. On site photographs of the trial pits. Additional figures of bacterial  
479 community composition and elemental ratios and solubility. Additional tables with full  
480 analytical results. Sequence reads have been uploaded to the National Center for  
481 Biotechnology Information (NCBI) under the Sequence Read Archive (SRA) accession  
482 number TBC. Collectively, the paper and these sources provide all the relevant data for  
483 this study.

#### 484 **Acknowledgements**

485 This research was funded by grant NE/L01405X/1 as part of the Resource  
486 Recovery from Waste programme administered by the Natural Environment Research  
487 Council (NERC), UK. The authors would like to thank Andy Connelly, Lesley Neve, Stephen  
488 Reid, Sheena Bennett, and David Elliott at the University of Leeds for technical support.

489

- 491 1. World Aluminium. World Aluminium — Alumina Production. (2017). Available at:  
492 <http://www.world-aluminium.org/statistics/alumina-production/>. (Accessed:  
493 26th May 2017)
- 494 2. Snars, K. & Gilkes, R. J. Evaluation of bauxite residues (red muds) of different  
495 origins for environmental applications. *Appl. Clay Sci.* **46**, 13–20 (2009).
- 496 3. International Aluminium Institute. *Bauxite Residue Management: Best Practice*  
497 *www.european-aluminium*. (2015).
- 498 4. Power, G., Gräfe, M. & Klauber, C. Bauxite residue issues: I. Current management,  
499 disposal and storage practices. *Hydrometallurgy* **108**, 33–45 (2011).
- 500 5. Hind, A. R., Bhargava, S. K. & Grocott, S. C. The surface chemistry of Bayer process  
501 solids: a review. *Colloids Surfaces A Physicochem. Eng. Asp.* **146**, 359–374 (1999).
- 502 6. Czop, M., Motyka, J., Sracek, O. & Szuwarzyński, M. Geochemistry of the  
503 Hyperalkaline Gorka Pit Lake (pH > 13) in the Chrzanow Region, Southern  
504 Poland. *Water, Air, Soil Pollut.* **214**, 423–434 (2011).
- 505 7. Mayes, W. M. *et al.* Dispersal and Attenuation of Trace Contaminants Downstream  
506 of the Ajka Bauxite Residue (Red Mud) Depository Failure, Hungary. *Environ. Sci.*  
507 *Technol.* **45**, 5147–5155 (2011).
- 508 8. Thornber, M. & Binet, D. Caustic Soda Adsorption on Bayer Residues. in *5th*  
509 *International Alumina Quality Workshop* (ed. Alumina Worsley) 498–507 (1999).
- 510 9. Menzies, N. W., Fulton, I. M., Kopittke, R. A. & Kopittke, P. M. Fresh Water Leaching  
511 of Alkaline Bauxite Residue after Sea Water Neutralization. *J. Environ. Qual.* **38**,  
512 2050 (2009).
- 513 10. Gräfe, M., Power, G. & Klauber, C. Bauxite residue issues: III. Alkalinity and  
514 associated chemistry. *Hydrometallurgy* **108**, 60–79 (2011).
- 515 11. Brunori, C., Cremisini, C., Massanisso, P., Pinto, V. & Torricelli, L. Reuse of a treated  
516 red mud bauxite waste: studies on environmental compatibility. *J. Hazard. Mater.*  
517 **117**, 55–63 (2005).
- 518 12. Burke, I. T. *et al.* Speciation of arsenic, chromium, and vanadium in red mud  
519 samples from the Ajka spill site, Hungary. *Environ. Sci. Technol.* **46**, 3085–3092  
520 (2012).
- 521 13. Klebercz, O. *et al.* Ecotoxicity of fluvial sediments downstream of the Ajka red  
522 mud spill, Hungary. *J. Environ. Monit.* **14**, 2063 (2012).
- 523 14. Lockwood, C. L. *et al.* Mobilisation of arsenic from bauxite residue (red mud)  
524 affected soils: Effect of pH and redox conditions. *Appl. Geochemistry* **51**, 268–277  
525 (2014).
- 526 15. Peacock, C. L. & Sherman, D. M. Vanadium(V) adsorption onto goethite ( $\alpha$ -FeOOH)  
527 at pH 1.5 to 12: a surface complexation model based on ab initio molecular  
528 geometries and EXAFS spectroscopy. *Geochim. Cosmochim. Acta* **68**, 1723–1733  
529 (2004).
- 530 16. Mamindy-Pajany, Y., Hurel, C., Marmier, N. & Roméo, M. Arsenic adsorption onto  
531 hematite and goethite. *Comptes Rendus Chim.* **12**, 876–881 (2009).
- 532 17. Renforth, P. *et al.* Contaminant mobility and carbon sequestration downstream of  
533 the Ajka (Hungary) red mud spill: The effects of gypsum dosing. *Sci. Total Environ.*  
534 **421**, 253–259 (2012).
- 535 18. Alcoa. *Pinjarra Refinery Long Term Residue Management Strategy*. (2011).
- 536 19. Alcoa. *Kwinana Refinery Long Term Residue Management Strategy*. (2012).

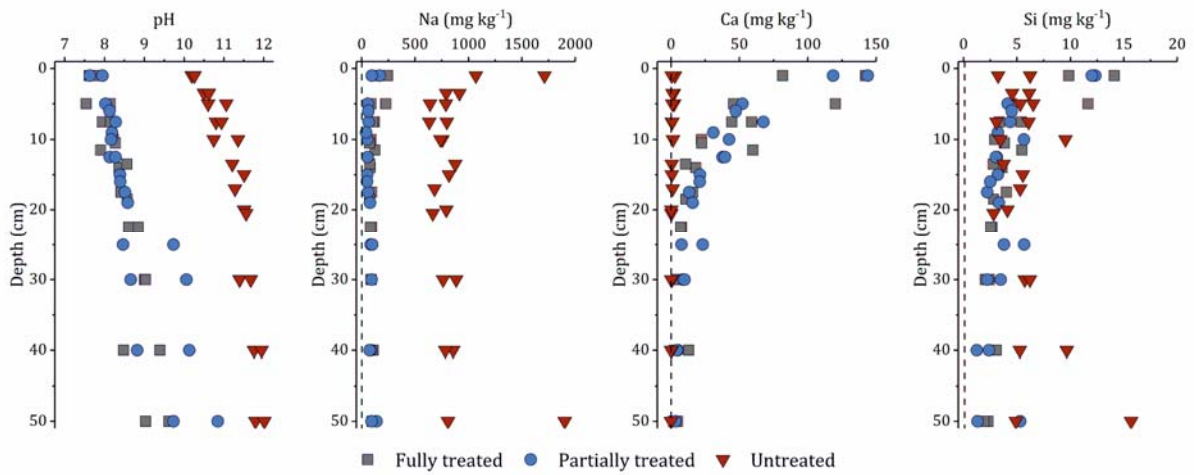
- 537 20. Burke, I. T. *et al.* Behavior of Aluminum, Arsenic, and Vanadium during the  
538 Neutralization of Red Mud Leachate by HCl, Gypsum, or Seawater. *Environ. Sci.*  
539 *Technol.* **47**, 6527–6535 (2013).
- 540 21. Lehoux, A. P. *et al.* Gypsum addition to soils contaminated by red mud:  
541 implications for aluminium, arsenic, molybdenum and vanadium solubility.  
542 *Environ. Geochem. Health* **35**, 643–656 (2013).
- 543 22. Kirwan, L. J., Hartshorn, A., McMonagle, J. B., Fleming, L. & Funnell, D. Chemistry of  
544 bauxite residue neutralisation and aspects to implementation. *Int. J. Miner.*  
545 *Process.* **119**, 40–50 (2013).
- 546 23. Hanahan, C. *et al.* Chemistry of Seawater Neutralization of Bauxite Refinery  
547 Residues (Red Mud). *Environ. Eng. Sci.* **21**, 125–138 (2004).
- 548 24. Wightman, G. & Davy Mckee Limited. Process for the removal of sodium values  
549 from sodium contaminated solids. (1994).
- 550 25. Kishida, M., Harato, T., Tokoro, C. & Owada, S. In situ remediation of bauxite  
551 residue by sulfuric acid leaching and bipolar-membrane electro dialysis.  
552 *Hydrometallurgy* **170**, 58–67 (2017).
- 553 26. Courtney, R., Timpson, J. P. & Grennan, E. Growth of *Trifolium pratense* in Red  
554 Mud Amended With Process Sand, Gypsum and Thermally Dried Sewage Sludge.  
555 *Int. J. Surf. Mining, Reclam. Environ.* **17**, 227–233 (2003).
- 556 27. Courtney, R. G. & Timpson, J. P. Nutrient status of vegetation grown in alkaline  
557 bauxite processing residue amended with gypsum and thermally dried sewage  
558 sludge - A two year field study. *Plant Soil* **266**, 187–194 (2004).
- 559 28. Courtney, R. G. & Timpson, J. P. Reclamation of Fine Fraction Bauxite Processing  
560 Residue (Red Mud) Amended with Coarse Fraction Residue and Gypsum. *Water.*  
561 *Air. Soil Pollut.* **164**, 91–102 (2005).
- 562 29. Courtney, R. G., Jordan, S. N. & Harrington, T. Physico-chemical changes in bauxite  
563 residue following application of spent mushroom compost and gypsum. *L. Degrad.*  
564 *Dev.* **20**, 572–581 (2009).
- 565 30. Courtney, R. & Mullen, G. Use of Germination and Seedling Performance Bioassays  
566 for Assessing Revegetation Strategies on Bauxite Residue. *Water. Air. Soil Pollut.*  
567 **197**, 15–22 (2009).
- 568 31. Courtney, R., Mullen, G. & Harrington, T. An evaluation of revegetation success on  
569 bauxite residue. *Restor. Ecol.* **17**, 350–358 (2009).
- 570 32. Courtney, R. & Harrington, T. Growth and nutrition of *Holcus lanatus* in bauxite  
571 residue amended with combinations of spent mushroom compost and gypsum. *L.*  
572 *Degrad. Dev.* **23**, 144–149 (2012).
- 573 33. Courtney, R. & Kirwan, L. Gypsum amendment of alkaline bauxite residue – Plant  
574 available aluminium and implications for grassland restoration - ScienceDirect.  
575 *Ecol. Eng.* **42**, 279–282 (2012).
- 576 34. Schmalenberger, A., O’Sullivan, O., Gahan, J., Cotter, P. D. & Courtney, R. Bacterial  
577 Communities Established in Bauxite Residues with Different Restoration  
578 Histories. *Environ. Sci. Technol.* **47**, 7110–7119 (2013).
- 579 35. Courtney, R., Feeney, E. & O’Grady, A. An ecological assessment of rehabilitated  
580 bauxite residue. *Ecol. Eng.* **73**, 373–379 (2014).
- 581 36. Courtney, R., Harris, J. A. & Pawlett, M. Microbial Community Composition in a  
582 Rehabilitated Bauxite Residue Disposal Area: A Case Study for Improving  
583 Microbial Community Composition. *Restor. Ecol.* **22**, 798–805 (2014).
- 584 37. Santini, T. C., Kerr, J. L. & Warren, L. A. Microbially-driven strategies for  
585 bioremediation of bauxite residue. *J. Hazard. Mater.* **293**, 131–157 (2015).

- 586 38. Zhu, F. *et al.* Natural plant colonization improves the physical condition of bauxite  
587 residue over time. *Environ. Sci. Pollut. Res.* **23**, 22897–22905 (2016).
- 588 39. Eaton, A. D., Clesceri, L. S., Rice, E. W. & Greenberg, A. E. *Standard Methods for the*  
589 *Examination of Water & Wastewater.* (American Public Health Association,  
590 2005).
- 591 40. Caporaso, J. G. *et al.* Global patterns of 16S rRNA diversity at a depth of millions of  
592 sequences per sample. *Proc. Natl. Acad. Sci. U. S. A.* **108 Suppl 1**, 4516–22 (2011).
- 593 41. Edgar, R. C. UPARSE: highly accurate OTU sequences from microbial amplicon  
594 reads. *Nat. Methods* **10**, 996–998 (2013).
- 595 42. Edgar, R. C. Search and clustering orders of magnitude faster than BLAST.  
596 *Bioinformatics* **26**, 2460–2461 (2010).
- 597 43. Yarza, P. *et al.* The All-Species Living Tree project: A 16S rRNA-based  
598 phylogenetic tree of all sequenced type strains. *Syst. Appl. Microbiol.* **31**, 241–250  
599 (2008).
- 600 44. Hill, M. O. Diversity and Evenness: A Unifying Notation and Its Consequences.  
601 *Ecology* **54**, 427–432 (1973).
- 602 45. Jost, L. Entropy and Diversity. *Oikos* **113**, 363–375 (2006).
- 603 46. Jost, L. PARTITIONING DIVERSITY INTO INDEPENDENT ALPHA AND BETA  
604 COMPONENTS. *Ecology* **88**, 2427–2439 (2007).
- 605 47. Kang, S., Rodrigues, J. L. M., Ng, J. P. & Gentry, T. J. Hill number as a bacterial  
606 diversity measure framework with high-throughput sequence data. *Sci. Rep.* **6**,  
607 38263 (2016).
- 608 48. Santini, T. C. Application of the Rietveld refinement method for quantification of  
609 mineral concentrations in bauxite residues (alumina refining tailings). *Int. J.*  
610 *Miner. Process.* **139**, 1–10 (2015).
- 611 49. Hertel, T., Blanpain, B. & Pontikes, Y. A Proposal for a 100% Use of Bauxite  
612 Residue Towards Inorganic Polymer Mortar. *J. Sustain. Metall.* **2**, 394–404 (2016).
- 613 50. Xue, S. *et al.* A review of the characterization and revegetation of bauxite residues  
614 (Red mud). *Environ. Sci. Pollut. Res.* **23**, 1120–1132 (2016).
- 615 51. Ruyters, S. *et al.* The Red Mud Accident in Ajka (Hungary): Plant Toxicity and  
616 Trace Metal Bioavailability in Red Mud Contaminated Soil. *Environ. Sci. Technol.*  
617 **45**, 1616–1622 (2011).
- 618 52. Buchman, M. F. *NOAA Screening Quick Reference Tables. NOAA OR&R Report 8-1*,  
619 (2008).
- 620 53. Barnes, M. C., Addai-Mensah, J. & Gerson, A. R. The mechanism of the sodalite-to-  
621 cancrinite phase transformation in synthetic spent Bayer liquor. *Microporous*  
622 *Mesoporous Mater.* **31**, 287–302 (1999).
- 623 54. Xu, H. & Van Deventer, J. S. J. The geopolymerisation of alumino-silicate minerals.  
624 *Int. J. Miner. Process.* **59**, 247–266 (2000).
- 625 55. Langmuir, D. *Aqueous environmental geochemistry.* (Prentice Hall, 1997).
- 626 56. Wehrli, B. & Stumm, W. Vanadyl in natural waters: Adsorption and hydrolysis  
627 promote oxygenation. *Geochim. Cosmochim. Acta* **53**, 69–77 (1989).
- 628 57. Genç, H., Tjell, J. C., McConchie, D. & Schuiling, O. Adsorption of arsenate from  
629 water using neutralized red mud. *J. Colloid Interface Sci.* **264**, 327–334 (2003).
- 630 58. Sherman, D. M. & Randall, S. R. Surface complexation of arsenic(V) to iron(III)  
631 (hydr)oxides: structural mechanism from ab initio molecular geometries and  
632 EXAFS spectroscopy. *Geochim. Cosmochim. Acta* **67**, 4223–4230 (2003).
- 633 59. TISDALL, J. M. & OADES, J. M. Organic matter and water-stable aggregates in soils.  
634 *J. Soil Sci.* **33**, 141–163 (1982).

- 635 60. Six, J., Paustian, K., Elliott, E. T. & Combrink, C. Soil Structure and Organic Matter.  
636 *Soil Sci. Soc. Am. J.* **64**, 681 (2000).
- 637 61. Six, J., Elliott, E. T. & Paustian, K. Soil Structure and Soil Organic Matter. *Soil Sci.*  
638 *Soc. Am. J.* **64**, 1042 (2000).
- 639 62. Knill, C. J. & Kennedy, J. F. Degradation of cellulose under alkaline conditions.  
640 *Carbohydr. Polym.* **51**, 281–300 (2003).
- 641 63. Humphreys, P. N., Laws, A. P. & Dawson, J. *A Review of Cellulose Degradation and*  
642 *the Fate of Degradation Products Under Repository Conditions.* (Nuclear  
643 Decommissioning Authority (NDA), 2010).
- 644 64. Rout, S. P. *et al.* Biodegradation of the alkaline cellulose degradation products  
645 generated during radioactive waste disposal. *PLoS One* **9**, e107433 (2014).
- 646 65. Fuller, R. D., Nelson, E. D. P. & Richardson, C. J. Reclamation of Red Mud (Bauxite  
647 Residues) Using Alkaline-Tolerant Grasses with Organic Amendments<sup>1</sup>. *J. Environ.*  
648 *Qual.* **11**, 533 (1982).
- 649 66. Wong, J. W. C. & Ho, G. Sewage sludge as organic ameliorant for revegetation of  
650 fine bauxite refining residue. *Resour. Conserv. Recycl.* **11**, 297–309 (1994).
- 651 67. Krüger, G. Verwitterungsversuche an Leuzit. *Chemie der Erde - Geochemistry* **12**,  
652 236–264 (1939).
- 653 68. Brady, P. V. & Walther, J. V. Controls on silicate dissolution rates in neutral and  
654 basic pH solutions at 25°C. *Geochim. Cosmochim. Acta* **53**, 2823–2830 (1989).
- 655 69. Hamilton, J. P., Brantley, S. L., Pantano, C. G., Criscenti, L. J. & Kubicki, J. D.  
656 Dissolution of nepheline, jadeite and albite glasses: toward better models for  
657 aluminosilicate dissolution. *Geochim. Cosmochim. Acta* **65**, 3683–3702 (2001).
- 658 70. Tole, M. P., Lasaga, A. C., Pantano, C. & White, W. B. The kinetics of dissolution of  
659 nepheline (NaAlSi<sub>3</sub>O<sub>8</sub>). *Geochim. Cosmochim. Acta* **50**, 379–392 (1986).
- 660 71. Oelkers, E. H. General kinetic description of multioxide silicate mineral and glass  
661 dissolution. *Geochim. Cosmochim. Acta* **65**, 3703–3719 (2001).
- 662 72. Álvarez-Ayuso, E. & Nugteren, H. W. Synthesis of dawsonite: A method to treat the  
663 etching waste streams of the aluminium anodising industry. *Water Res.* **39**, 2096–  
664 2104 (2005).
- 665 73. Schlesinger, W. H. & Andrews, J. A. Soil respiration and the global carbon cycle.  
666 *Biogeochemistry* **48**, 7–20 (2000).
- 667 74. Zhou, J., Bruns, M. A. & Tiedje, J. M. DNA recovery from soils of diverse  
668 composition. *Appl. Environ. Microbiol.* **62**, 316–322 (1996).
- 669 75. Krishna, P., Babu, A. G. & Reddy, M. S. Bacterial diversity of extremely alkaline  
670 bauxite residue site of alumina industrial plant using culturable bacteria and  
671 residue 16S rRNA gene clones. *Extremophiles* **18**, 665–676 (2014).
- 672 76. Müller, D. B., Vogel, C., Bai, Y. & Vorholt, J. A. The Plant Microbiota: Systems-Level  
673 Insights and Perspectives. *Annu. Rev. Genet.* **50**, 211–234 (2016).
- 674 77. Bulgarelli, D. *et al.* Revealing structure and assembly cues for Arabidopsis root-  
675 inhabiting bacterial microbiota. *Nature* **488**, 91–95 (2012).
- 676 78. Lundberg, D. S. *et al.* Defining the core Arabidopsis thaliana root microbiome.  
677 *Nature* **488**, 86–90 (2012).
- 678 79. Jones, R. T. *et al.* A comprehensive survey of soil acidobacterial diversity using  
679 pyrosequencing and clone library analyses. *ISME J.* **3**, 442–53 (2009).
- 680 80. Liu, W., Zhang, W., Liu, G., Zhang, Y. & Zhang, G. Microbial diversity in the saline-  
681 alkali soil of a coastal Tamarix chinensis woodland at Bohai Bay, China. *J. Arid*  
682 *Land* **8**, 284–292 (2016).
- 683 81. Huber, K. J. *et al.* The first representative of the globally widespread subdivision 6

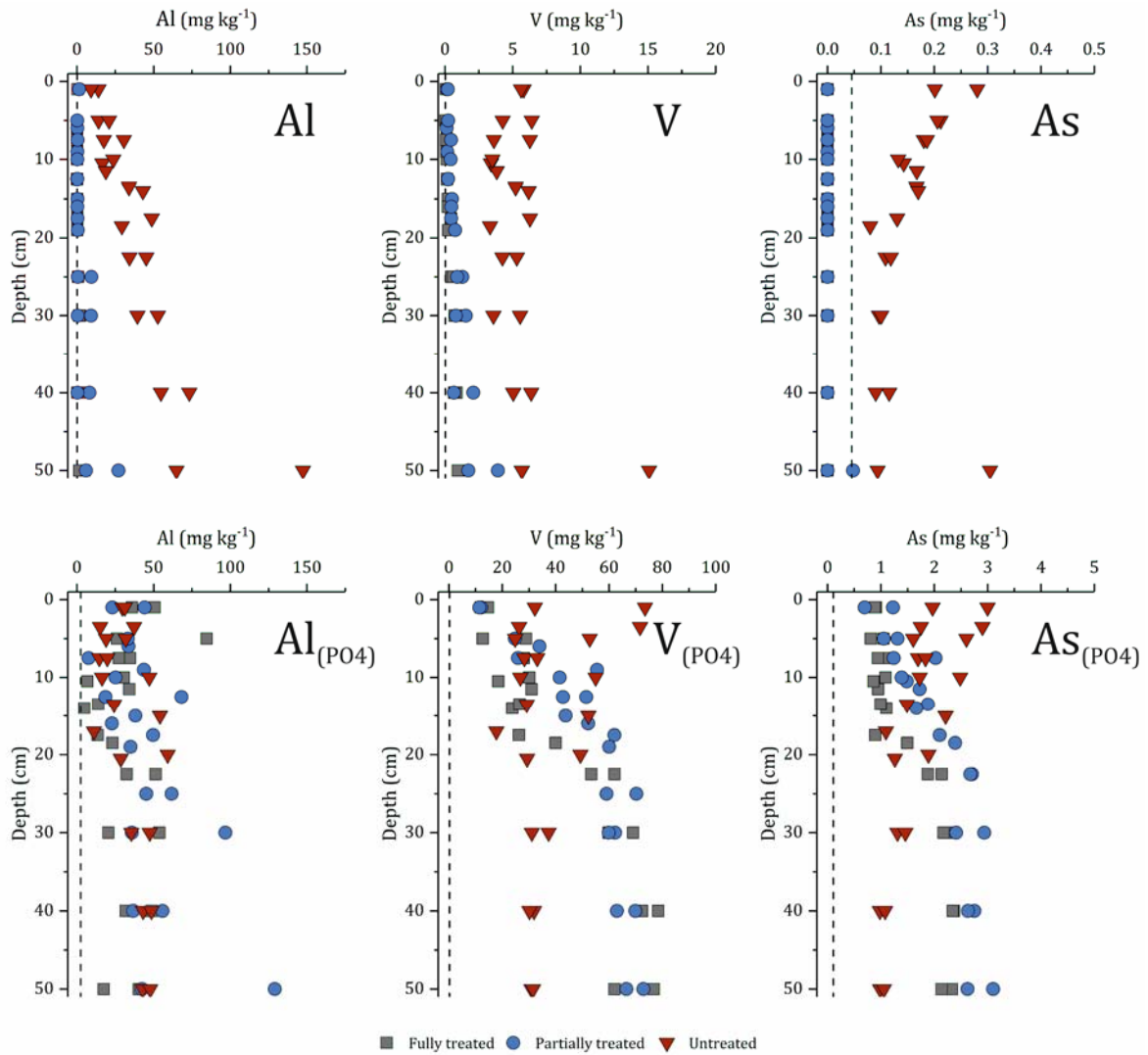
- 684 Acidobacteria, *Vicinamibacter silvestris* gen. nov., sp. nov., isolated from  
685 subtropical savannah soil. *Int. J. Syst. Evol. Microbiol.* **66**, 2971–2979 (2016).
- 686 82. Li, X., Sun, M., Zhang, H., Xu, N. & Sun, G. Use of mulberry–soybean intercropping  
687 in salt–alkali soil impacts the diversity of the soil bacterial community. *Microb.*  
688 *Biotechnol.* **9**, 293–304 (2016).
- 689 83. Lage, O. M. & Bondoso, J. Bringing Planctomycetes into pure culture. *Front.*  
690 *Microbiol.* **3**, 405 (2012).
- 691 84. Chistoserdova, L. *et al.* The Enigmatic Planctomycetes May Hold a Key to the  
692 Origins of Methanogenesis and Methylophony. *Mol. Biol. Evol.* **21**, 1234–1241  
693 (2004).
- 694 85. Scheuner, C. *et al.* Complete genome sequence of *Planctomyces brasiliensis* type  
695 strain (DSM 5305T), phylogenomic analysis and reclassification of  
696 Planctomycetes including the descriptions of *Gimesia* gen. nov., *Planctopirus* gen.  
697 nov. and *Rubinisphaera* gen. nov. and emended descriptions of the order  
698 Planctomycetales and the family Planctomycetaceae. *Stand. Genomic Sci.* **9**, 10  
699 (2014).
- 700 86. Ferreira, C., Soares, A. R., Lamosa, P., Santos, M. A. & da Costa, M. S. Comparison of  
701 the compatible solute pool of two slightly halophilic planctomycetes species,  
702 *Gimesia maris* and *Rubinisphaera brasiliensis*. *Extremophiles* **20**, 811–820 (2016).
- 703 87. Elshahed, M. S. *et al.* Phylogenetic and metabolic diversity of Planctomycetes from  
704 anaerobic, sulfide- and sulfur-rich Zodletone Spring, Oklahoma. *Appl. Environ.*  
705 *Microbiol.* **73**, 4707–16 (2007).
- 706
- 707

708 **Figures.**



709  
710  
711  
712  
713  
714

**Figure 1.** pH, Na, Si, and Ca aqueously extracted from fully treated, partially treated, and untreated bauxite residue as a function of depth. The dotted line represents the limit of detection for element.

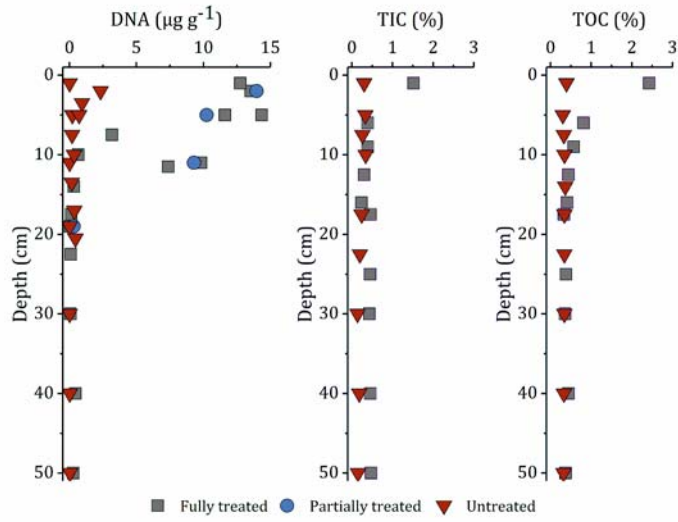


715  
716  
717  
718  
719  
720  
721

**Figure 2.**

Concentrations of Al, V, and As in solution following aqueous and phosphate (PO4) extractions from fully treated, partially treated, and untreated bauxite residue as a function of depth. Note the change in x-axis scale for aqueous and phosphate extracted V and As. The dotted line represents the limit of detection for each element.





722  
723  
724  
725  
726

**Figure 3.**

DNA, total inorganic carbon (TIC), and total organic carbon (TOC) concentrations in fully treated, partially treated, and untreated bauxite residue as a function of depth.

727  
728  
729  
730

**Table 1.**

Semi-quantitative percentage of crystalline phases present in bauxite residue as a function of treatment and average across depth, fitted using Rietveld refinement. Uncertainty on the Rietveld refinement is approximately 5 %. Full details are available in Table S2.

Treatment site	Fe Oxyhydroxides		Al oxyhydroxides			Desilication Products		Ti Oxides	Other minerals
	Goethite	Hematite	Gibbsite	Boehmite	Katoite	Cancrinite	Sodalite	Perovskite	
	$\alpha$ -FeO(OH)	Fe <sub>2</sub> O <sub>3</sub>	Al(OH) <sub>3</sub>	$\gamma$ -AlO(OH)	Ca <sub>3</sub> Al <sub>2</sub> (OH) <sub>12</sub>	Na <sub>6</sub> Ca <sub>2</sub> Al <sub>6</sub> Si <sub>6</sub> O <sub>24</sub> (CO <sub>3</sub> ) <sub>2</sub>	Na <sub>8</sub> Al <sub>6</sub> Si <sub>6</sub> O <sub>24</sub> (OH) <sub>2</sub>	CaTiO <sub>3</sub>	
	%	%	%	%	%	%	%	%	
Untreated	21	16	8	10	2	14	1	20	9
Fully Treated	24	19	8	7	3	10	< 0.5	20	9
Partially Treated	19	16	11	10	10	10	< 0.5	15	8

731  
732